Sampling on the Sierpinski Gasket

Richard Oberlin, Brian Street, and Robert S. Strichartz

CONTENTS

We study regular and irregular sampling for functions defined on the Sierpinski Gasket (SG), where we interpret "bandlimited" to mean the function has a finite expansion in the first d_m Dirichlet eigenfunctions of the Laplacian as defined by Kigami, and d_m is the cardinality of the sampling set. In the regular case, we take the sampling set to be the nonboundary vertices of the level m graph approximating SG. We prove that regular sampling is always possible, and we give an algorithm to compute the sampling functions, based on an extension of the spectral decimation method of Fukushima and Shima to include inner products. We give experimental evidence that the sampling functions decay rapidly away from the sampling point, in striking contrast to the classical theory on the line where the sinc function exhibits excruciatingly slow decay. Similar behavior appears to hold for certain Dirichlet kernels. We show by example that the sampling formula provides an appealing method of approximating functions that are not necessarily bandlimited, and so might be useful for numerical analysis. We give experimental evidence that reasonable perturbations of one of the regular sampling sets remains a sampling set. In contrast to what happens on the unit interval, it is not true that all sets of the correct cardinality are sampling sets.

1. INTRODUCTION

Sampling is the process of "connecting the dots." A function is given at a discrete set of points (the *sample* values), and it is assumed that it is *bandlimited*, meaning that its natural spectral expansion only lives on a bottom interval of the spectrum. Then an explicit formula, the *sampling formula*, gives the function in terms of its sample values and certain *sampling functions*; generically, we write

$$f(x) = \sum_{y \in S} f(y)\psi_y(x) \quad \text{for} \quad f \in B, \qquad (1\text{–}1)$$

where S is the sampling set, B is the space of bandlimited functions, and ψ_y are the sampling functions.

In the classical Shannon-Whittaker sampling theorem, the underlying space is the real line, the bandlimited

2000 AMS Subject Classification: Primary; 28A80, 42C99, 94A20

Keywords: Sierpinski gasket, sampling theory, Dirichlet kernel, analysis on fractals, spectral decimation

1058-6458/2003 $0.50 per page

functions B are the L^2 functions whose Fourier transform is supported in an interval $|\lambda| \le b$,

$$f(x) = \int_{-b}^{b} e^{-2\pi i \lambda x} \widehat{f}(\lambda) d\lambda, \tag{1–2}$$

S is the lattice $b^{-1}\mathbb{Z}$, and $\psi_y(x)$ is a translate of the sinc function (when $b = 1$),

$$\text{sinc } x = \frac{\sin \pi x}{\pi x}. \tag{1–3}$$

The sluggish decay of this function means that the sampling formula converges very slowly. In practice, various strategies are used to deal with this, such as oversampling by taking a tighter lattice, involving redundancy of the sample data. The book [Benedetto and Ferreira 01] gives an overview of recent research in this area.

A simple variant of this theorem deals with the unit interval as the underlying space, and either Fourier sine or cosine expansions. We describe the situation for sine series, which means eigenfunctions of the Laplacian (second derivative) with Dirichlet boundary conditions, but the other case is essentially the same. We assume all functions we deal with vanish on the boundary. Choose a number m, and define B_m to be the functions of the form

$$f(x) = \sum_{k=1}^{m} \widehat{f}(k) \sin \pi k x. \tag{1–4}$$

For our regular sampling set S_m, we take the numbers of the form $k/(m+1)$, $k = 1, \ldots, m$. It is not hard to see that

$$\psi_y^{(m)}(x) = \frac{4}{2m+1} \sum_{k=1}^{m} \sin \pi k y \sin \pi k x \quad \text{for} \quad y \in S_m \tag{1–5}$$

is a function of the form (1–4) that satisfies

$$\psi_y^{(m)}(x) = \delta(x, y) \quad \text{for} \quad x, y \in S_m \tag{1–6}$$

so that (1–1) holds, and moreover,

$$\psi_y^{(m)}(x) = \frac{1}{2m+1} \frac{\sin \frac{\pi}{2}(2m+1)(x-y)}{\sin \frac{\pi}{2}(x-y)} - \frac{1}{2m+1} \frac{\sin \frac{\pi}{2}(2m+1)(x+y)}{\sin \frac{\pi}{2}(x+y)}. \tag{1–7}$$

Note that the first term on the right side of (1–7) is just $\frac{1}{2m+1} D_m(x-y)$ where D_m is the standard Dirichlet kernel for Fourier series, and the second term is a relatively small correction term. Results very closely related to this may be found in [Cauchy 41].

In this paper, we will study the analogous situation on the Sierpinski gasket (SG), which can be thought of as a fractal analog of the unit interval. There is a well developed theory of a Laplacian and related analytic and stochastic constructs, as described in the books [Kigami 01] and [Barlow 98], and the expository article [Strichartz 99]. For the Laplacian constructed in [Kigami 89], there is a complete description of its spectrum in [Fukushima and Shima 92], which was further elaborated in [Dalrymple et al. 99] and [Gibbons et al. 01], so that it is possible to describe bandlimited functions precisely.

We now give a brief outline of the theory. We treat SG as a limit of graphs Γ_m with vertices V_m and edge relation $x \sim_m y$ defined inductively as follows. Γ_0 is the complete graph on V_0 consisting of the three vertices (q_0, q_1, q_2) of an equilateral triangle in the plane. We consider V_0 to be the boundary of SG and all the graphs Γ_m. Let F_i denote the contractive similarity with fixed point q_i and contraction ratio $1/2$. Note that

$$SG = \bigcup_{i=0}^{2} F_i(SG), \tag{1–8}$$

and is, in fact, the unique nonempty compact set satisfying (1–8). We then set

$$V_m = \bigcup_{i=0}^{2} F_i(V_{m-1}) \tag{1–9}$$

and connect $x \sim_m y$ if there exist i and $x', y' \in V_{m-1}$ with $x' \sim_{m-1} y'$ and $x = F_i x'$, $y \in F_i y'$. Note that $\#V_m = \frac{1}{2}(3^{m+1} + 3)$. We also write $F_w = F_{w_1} \cdots F_{w_m}$ for w a word $(w_1, \ldots, w_m)$ of length $|w| = m$, and call $F_w(SG)$ a *cell* of order m. The set $V_* = \cup V_m$ of all vertices is dense in SG, so a continuous function on SG is determined by its values on V_*.

The Laplacian Δ (strictly speaking, we should call this the symmetric Laplacian, since there are other possible choices) may be defined pointwise by

$$\Delta u(x) = \lim_{m \to \infty} \frac{3}{2} 5^m \Delta_m u(x) \quad x \in V_* \setminus V_0, \tag{1–10}$$

where Δ_m denotes the graph Laplacian

$$\Delta_m u(x) = \sum_{y \sim_m x} (u(y) - u(x)) \quad \text{for} \quad x \in V_m \setminus V_0 \tag{1–11}$$

(note that there are exactly four points y connected to a fixed x in $V_m \setminus V_0$). Here, we require that both u and Δu be continuous functions and the limit (1–10) be uniform. There is also a weak formulation of the Laplacian,

which explains the factor 3/2 and the renormalization coefficient 5^m in (1–10) (please note that some references inadvertantly omit the factor 3/2, but this does not materially affect anything).

The Laplacian is a negative self-adjoint operator on $L^2(SG)$ with respect to the normalized Hausdorff measure (each cell of order m has measure 3^{-m}) and Dirichlet boundary conditions (vanishing on V_0) and $L^2(SG)$ has an orthonormal basis $\{\widetilde{u}_j(x)\}$ of eigenfunctions of increasing eigenvalues, although many eigenspaces have large multiplicities. We postpone a detailed description of the eigenfunctions until Section 2. Also, there is an analogous theory of Neumann eigenfunctions, but for simplicity we will deal with the Dirichlet case exclusively. We define the space B_m to be the span of the first d_m eigenfunctions (counting multiplicity), where $d_m = \frac{1}{2}(3^m - 3)$. This number is chosen because $\#(V_m \setminus V_0) = d_m$, and $V_m \setminus V_0$ will serve as our regular sampling set. We will show in Section 2 that a formula analogous to (1–5) holds in this context. To turn this into an effective algorithm for computing the sampling functions, we need to establish a rather technical lemma (Lemma 2.2) concerning inner products of eigenfunctions on the graphs Γ_m. The method of Fukushima and Shima is called *spectral decimation* because it relates the spectra of the discrete Laplacians Δ_m on the graphs Γ_m and the Laplacian Δ on the fractal limit, both eigenvalues and eigenfunctions. Our result adds one more chapter to this story. There is a class of fractals described in [Shima 96] for which the spectral decimation method holds. It is likely that our result also extends to this class of fractals, but this has yet to be demonstrated.

Once we have in place an effective algorithm for computing the sampling functions, we are able to carry out some interesting numerical experiments. In Section 3, we describe some of the results concerning the sampling functions. The most striking is the apparent strong localization of these functions: $\psi_y^{(m)}(x)$ decays very rapidly as x moves away from y. One of the startling results of [Fukushima and Shima 92] is the existence of localized eigenfunctions, a phenomenon that is further developed in [Barlow and Kigami 97]. Our conjectured result seems to be one more facet of this localization principle. We also show the same conjectural localization for the Dirichlet kernel for the analogous partial sums of the eigenfunction expansions,

$$D_{d_m}(x,y) = \sum_{j=1}^{d_m} \widetilde{u}_j(x)\widetilde{u}_j(y) \qquad (1\text{–}12)$$

(this would be the analog of a lacunary subsequence of ordinary Dirichlet kernels). Although our results are conjectural for all m, they are clearly established for $m \le 5$, and it should be kept in mind that in sampling theory, one is not usualy concerned with the limit as $m \to \infty$, but with rather modest values of m. We also find experimental evidence for a splitting analogous to (1–7) of the sampling function into an "ideal spike" independent of y and a correction term.

In Section 4, we discuss the use of the sampling formula as a method of approximation for functions that are not bandlimited. We give experimental evidence that this method works quite well. This suggests the possibility of developing a form of numerical analysis on SG based on the sampling approximation. It is not clear how well this would perform in comparison with the spline and finite element method as developed in [Strichartz and Usher 00] and [Gibbons et al. 01], but it might be worth investigating in connection with the wave equation, which was investigated using a rather crude finite difference method in [Dalrymple et al. 99].

In Section 5, we investigate irregular sampling, where we keep the bandlimited space B_m, but change the sampling set. The situation is quite different from the unit interval, where any sampling set of the correct cardinality will do. We give some experimental evidence that any reasonably small perturbation of $V_m \setminus V_0$ can serve as a sampling set, which is similar to the sitution on the real line.

The web site, http://www.mathlab.cornell.edu/~brian/sampling/, contains all the programs used in our experiments and more data in both numerical and graphical form.

2. REGULAR SAMPLING

We begin with a generic observation about sampling for a finite dimensional space B of functions on a set K and a finite sampling set $S \subseteq K$. We assume the dimension d of B is equal to the cardinality of S, and the functions in B when restricted to S still form a d dimensional space. (For simplicity of notation, we deal with real valued functions.) A set of *sampling functions* $\psi_y \in B$ for each $y \in S$ is a solution to the problem

$$\psi_y(x) = \delta(y,x) \quad \text{for all} \quad x \in S. \qquad (2\text{–}1)$$

This implies the sampling formula

$$f(x) = \sum_{y \in S} f(y)\psi_y(x) \quad \text{for all} \quad f \in B. \qquad (2\text{–}2)$$

Proposition 2.1. *Let $\{u_j\}$ be an orthonormal basis for B with respect to the $\ell^2(S)$ inner product, namely*

$$\sum_{x\in S} u_j(x)u_k(x) = \delta_{j,k}. \tag{2–3}$$

Then

$$\psi_y(x) = \sum_{j=1}^{d} u_j(y)u_j(x) \quad \textit{for} \quad y \in S \tag{2–4}$$

gives a set of sampling functions, and it is unique.

Proof: Regard $\{u_j(x)\}$ as a $d \times d$ matrix. Then (2–3) is orthonormality of (say) rows, and (2–1) for $\psi_y(x)$ given by (2–4) is orthonormality of columns. Also it is clear that existence and uniqueness of solutions of (2–1) are equivalent by the fundamental theorem of linear algebra. □

We now turn to the specific context of regular sampling on SG, when we take the sampling set to be $V_m \setminus V_0$, of cardinality $d_m = \frac{1}{2}(3^{m+1} - 3)$, and the space of functions B_m to be the span of the Dirichlet eigenfunctions of Δ for the lowest d_m eigenvalues. In the notation of [Gibbons et al 2001], these are all the eigenvalues up to $5^{m-2}\lambda_1^{(6)}$ (for $m \geq 2$). According to [Fukushima and Shima 92], every Dirichlet eigenfunction of the discrete Laplacian Δ_m on V_m extends in infinitely many ways to a Dirichlet eigenfunction on SG, and if we collect the extensions with lowest eigenvalues, we obtain exactly B_m. In particular, the hypothesis that the restrictions of B_m functions to $V_m \setminus V_0$ have dimension d_m is valid. Moreover, eigenfunctions in B_m corresponding to distinct eigenvalues of Δ on SG remain orthogonal with respect to the $\ell^2(V_m)$ inner product since they are eigenfunctions of Δ_m with distinct eigenvalues (the fact that the eigenvalues remain distinct is only valid among the eigenfunctions in B_m, of course).

So our primary problem in computing the sampling functions is to find an orthonormal basis within each eigenspace for the $\ell^2(V_m)$ inner product. We are also interested in the relation between the $\ell^2(V_m)$ and $L^2(SG)$ inner products. It turns out that they are simply scalar multiples of each other, and we can compute the scalar more or less explicitly. This is significant because many of the eigenspaces have high multiplicity.

We now briefly recapitulate the results of [Fukushima and Shima 92], as elaborated in [Dalrymple et al. 99]. For each Dirichlet eigenvalue λ of Δ on SG, there is a number $k \geq 1$, the "generation of birth," such that every eigenfunction f in the λ-eigenspace E_λ, when restricted to V_k, is an eigenfunction of Δ_k with eigenvalue 2, 5, or 6. There is the additional restriction that 2 occurs only for $k = 1$, while 6 occurs only for $k > 1$. Thereafter, the restrictions of f to V_m are determined by the restriction to V_{m-1} by a simple local linear extension algorithm. These algorithms are controlled by the choice of a sequence $(\varepsilon_1, \varepsilon_2, \ldots)$ where each ε_j is ± 1, and all but a finite number are -1 (in addition, if the initial eigenvalue is 6, then $\varepsilon_1 = +1$ only). The restriction of f to V_m for $m > k$ becomes an eigenfunction of Δ_m with eigenvalue λ_m given by

$$\lambda_m = \frac{1}{2}(5 + \varepsilon_{m-k}\sqrt{25 - 4\lambda_{m-1}}). \tag{2–5}$$

Note that this means

$$\lambda_{m-1} = \lambda_m(5 - \lambda_m), \tag{2–6}$$

and ε_{m-k} simply chooses one of the roots of the quadradic equation (2–6). The eigenvalue λ on SG is related to these values by

$$\lambda = \frac{3}{2}\lim_{m\to\infty} 5^m\lambda_m, \tag{2–7}$$

the condition that all but a finite number of ε_j equal -1 guaranteeing that the limit exists.

To describe the extension algorithm, we adopt the following flexible notation. Let v be a vertex in V_m that is not in V_{m-1}. Then v belongs to a cell of level $m-1$, and we denote by v_0 and v_1 the vertices of this cell closest to v, and v_2 the vertex opposite v. Then

$$f(v) = \frac{(4-\lambda_m)}{(2-\lambda_m)(5-\lambda_m)}(f(v_0) + f(v_1)) + \frac{2}{(2-\lambda_m)(5-\lambda_m)}f(v_2) \tag{2–8}$$

(see [Dalrymple et al. 99, Algorithm 2.4]).

Let $\|f\|_m$ and $\langle f, g\rangle_m$ denote the $\ell^2(V_m)$ norm and inner product. Since the cardinality of V_m grows on the order of 3^m, we would expect $\|f\|_m^2$ to grow roughly the same. It is easy to see that

$$\|f\|^2 = \frac{2}{3}\lim_{m\to\infty} 3^{-m}\|f\|_m^2 \text{ for continuous } f, \tag{2–9}$$

where $\|f\|$ and $\langle f, g\rangle$ denote the $L^2(SG)$ norm and inner product.

Lemma 2.2. *For f in E_λ,*

$$\|f\|_m^2 = \frac{(6-\lambda_m)(5-2\lambda_m)}{(5-\lambda_m)(2-\lambda_m)}\|f\|_{m-1}^2 \quad \textit{for} \quad m > k. \tag{2–10}$$

Remark 2.3. The coefficient in (2–10) is always positive, since $0 < \lambda_m < 5$ and either $\lambda_m < 2$ or $\lambda_m > 5/2$. Also, the coefficient tends to 3 as $m \to \infty$ because $\lambda_m \to 0$.

Proof of Lemma 2.2: Clearly,

$$\|f\|_m^2 = \|f\|_{m-1}^2 + \sum_{x \in V_m \setminus V_{m-1}} |f(x)|^2. \tag{2–11}$$

We substitute (2–8) into the last sum. Let

$$a = \frac{4 - \lambda_m}{(2 - \lambda_m)(5 - \lambda_m)}$$

and

$$b = \frac{2}{(2 - \lambda_m)(5 - \lambda_m)}.$$

Then we have

$$\sum_{x \in V_m \setminus V_{m-1}} |f(x)|^2 = 2(2a^2 + b^2)\|f\|_{m-1}^2 + 2(a^2 + 2ab) \sum_{x \sim_{m-1} y} f(x)f(y) \tag{2–12}$$

because each $x \in V_{m-1} \setminus V_0$ belongs to two cells of level $m - 1$.

To eliminate the last term in (2–12), we use the fact that f is an eigenfunction for Δ_{m-1} with eigenvalue λ_{m-1}. In the weak formulation, this means

$$\sum_{x \sim_{m-1} y} |f(x) - f(y)|^2 = 4\|f\|_{m-1}^2 - 2 \sum_{x \sim_{m-1} y} f(x)f(y) = \lambda_{m-1}\|f\|_{m-1}^2,$$

and so

$$\sum_{x \sim_{m-1} y} f(x)f(y) = \frac{1}{2}(4 - \lambda_{m-1})\|f\|_{m-1}^2. \tag{2–13}$$

Combining (2–11), (2–12), and (2–13), we obtain

$$\|f\|_m^2 = (1 + 2(2a^2 + b^2) + (4 - \lambda_{m-1})(a^2 + 2ab))\|f\|_{m-1}^2. \tag{2–14}$$

It remains to identify the coefficient in (2–14) with the coefficient in (2–10). Using (2–6), we have $4 - \lambda_{m-1} = (1 - \lambda_m)(4 - \lambda_m)$, so the coefficient in (2–14) becomes

$$1 + 2(2a^2 + b^2) + (1 - \lambda_m)(4 - \lambda_m)a(a + 2b), \tag{2–15}$$

an expression involving λ_m alone. The rest is algebra. Note that

$$\begin{aligned} &2(2a^2 + b^2) + (1 - \lambda_m)(4 - \lambda_m)a(a + 2b) \\ &\quad = \frac{72 - 32\lambda_m + 4\lambda_m^2}{(2 - \lambda_m)^2(5 - \lambda_m)^2} \\ &\qquad + \frac{(128 - 208\lambda_m + 96\lambda_m^2 - 17\lambda_m^3 + \lambda_m^4)}{(2 - \lambda_m)^2(5 - \lambda_m)^2} \\ &\quad = \frac{200 - 240\lambda_m + 100\lambda_m^2 - 17\lambda_m^3 + \lambda_m^4}{(2 - \lambda_m)^2(5 - \lambda_m^2)} \\ &\quad = \frac{20 - 10\lambda_m + \lambda_m^2}{(2 - \lambda_m)(5 - \lambda_m)}. \end{aligned}$$

Thus, (2–15) becomes

$$\frac{10 - 7\lambda_m + \lambda_m^2 + (20 - 10\lambda_m + \lambda_m^2)}{(2 - \lambda_m)(5 - \lambda_m)} = \frac{30 - 17\lambda_m + 2\lambda_m^2}{(2 - \lambda_m)(5 - \lambda_m)} = \frac{(6 - \lambda_m)(5 - 2\lambda_m)}{(2 - \lambda_m)(5 - \lambda_m)}$$

as desired. □

To simplify the notation, we define

$$b(t) = \frac{(1 - \frac{1}{6}t)(1 - \frac{2}{5}t)}{(1 - \frac{1}{5}t)(1 - \frac{1}{2}t)}. \tag{2–16}$$

Note that

$$b(t) = 1 + \frac{2}{15}t + O(t^2) \quad \text{as} \quad t \to 0. \tag{2–17}$$

Then (2–10) can be written

$$\|f\|_m^2 = 3b(\lambda_m)\|f\|_{m-1}^2 \quad \text{for} \quad m > k. \tag{2–18}$$

Corollary 2.4. *Let k be the generation of birth of λ. For $f, g \in E_\lambda$, and $m > k$,*

$$\langle f, g\rangle_m = 3^{m-k}\Big(\prod_{j=k+1}^{m} b(\lambda_j)\Big)\langle f, g\rangle_k. \tag{2–19}$$

Also

$$\langle f, g\rangle = 2 \cdot 3^{-k-1}\Big(\prod_{j=k+1}^{\infty} b(\lambda_j)\Big)\langle f, g\rangle_k. \tag{2–20}$$

Proof: Equation (2–19) follows from (2–18) by polarization and iteration. Using (2–9), we may take the limit as $m \to \infty$ to obtain (2–20). Note that the convergence of the infinite product in (2–20) is guaranteed by (2–17) and the estimate $\lambda_n = O(5^{-n})$ for large n, a consequence of (2–7). □

We can now describe an algorithm for finding an orthonormal basis for E_λ with respect to the $\ell^2(V_m)$ inner product, assuming $k \le m$ (this holds for the first d_m eigenvalues, the only ones in which we are interested).

Step 1. Find an orthonormal basis for the $\ell^2(V_k)$ inner product.

Step 2. Multiply each basis element by the factor

$$\Big(3^{m-k} \prod_{j=k+1}^{m} b(\lambda_j)\Big)^{-1/2}.$$

Step 1 is essentially an ad hoc procedure. Start with any basis and apply Gram-Schmidt. The important point to note is that, for each fixed k, there are only two such computations, $\lambda_1 = 2$ or 5 and $\lambda_k = 5$ or 6 for $k \ge 2$. When $\lambda_1 = 2$, the eigenspace is simple, but for $\lambda_k = 5$ or 6, the multiplicity grows exponentially in k. Explicit bases are given in [Dalrymple et al 1999]. An implementation of this algorithm may be found on the web site. For our computations, we were able to take values up to $m = 5$, and computed values on V_8.

Using Corollary 2.3, it is not hard to transform an orthonormal basis for B_m with respect to the $\ell^2(V_m)$ inner product into an orthonormal basis with respect to the $L^2(SG)$ inner product. This is significant because if we use such a basis on the right side of (2–4), we obtain the Dirichlet kernel $D_{d_m}(x, y)$ for finding the partial sums (of order d_m) of the Dirichlet eigenfunction expansion of an arbitrary function f as

$$\int_{SG} D_{d_m}(x, y) f(y) d\mu(y). \tag{2–21}$$

In fact, once we have computed an orthonormal basis for E_λ with respect to $\ell^2(V_m)$, we just have to multiply each basis element by the factor

$$\Big(2 \cdot 3^{-m-1} \prod_{j=m+1}^{\infty} b(\lambda_j)\Big)^{-1/2}. \tag{2–22}$$

Note that the infinite product in (2–22) is a function of λ_m alone,

$$\widetilde{b}(\lambda_m) = \prod_{j=m+1}^{\infty} b(\lambda_j), \tag{2–23}$$

because each λ_j for $j > m$ is given by

$$\lambda_j = \frac{1}{2}(5 - \sqrt{25 - 4\lambda_{j-1}}), \tag{2–24}$$

the choice $\varepsilon = -1$ in (2–5). An approximation to $\widetilde{b}$ is easily computed; see Figure 1.

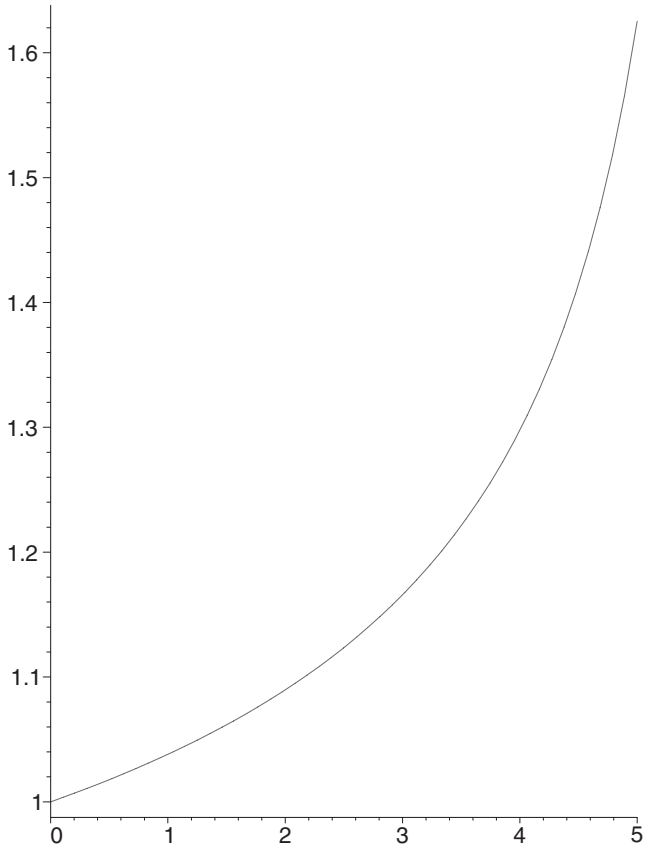

FIGURE 1. An approximate graph of the function $\widetilde{b}$.

3. PROPERTIES OF THE SAMPLING FUNCTIONS AND DIRICHLET KERNELS

Using the algorithms described in the previous section, we computed all the sampling functions $\psi_y^{(m)}$ for $1 \le m \le 5$. In Figure 2, we display the graphs for $m = 2$ (although there are a total of 12 points in $V_2 \setminus V_0$, the sampling functions fall into just three orbits under the symmetry group D_3, so it suffices to show just 3 graphs). In Figure 3, we display the sequence of graphs $\psi_y^{(m)}$ for a fixed $y \in V_1 \setminus V_0$ and $m = 1, \ldots, 5$. In Figure 4, we display $\psi_y^{(5)}$ for several choices of $y \in V_5$. It is easy to locate the point y visually on the graphs since it is the unique point in V_m where ψ_y is nonzero ($\psi_y(y) = 1$), and the function assumes its maximum value close to y. Our data indicate a maximum value of about 1.04 for some choices of y, attained at a point quite close to y.

Since $\psi_y^{(m)}(x) = 0$ for $x \in V_m$, $x \ne y$, it is possible for $\psi_y^{(m)}$ to "change sign" in a neighborhood of such points. An ideal manifestation of this phenomenon would be if $\psi_y^{(m)}$ had a constant sign on each component of $(SG \setminus V_m) \cup \{y\}$, with opposite signs on neighboring components. Our data shows that this does not hold exactly,

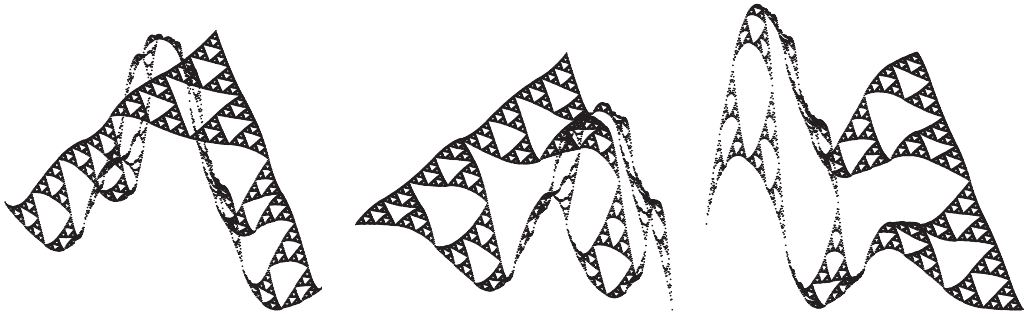

(a) (b) (c)

FIGURE 2. The graphs of $\psi_y^{(2)}$ for three different choices of $y \in V_2$.

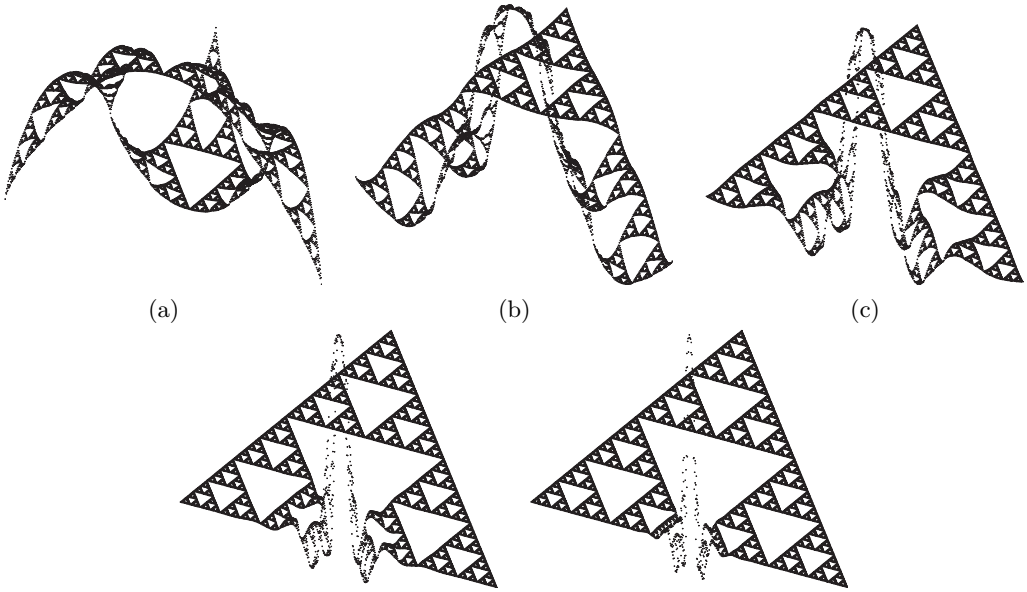

(a) (b) (c)

(d) (e)

FIGURE 3. The graphs of $\psi_y^{(m)}$ for $m = 1, 2, 3, 4, 5$ for y fixed in $V_1 \setminus V_0$.

but is approximately true. In Figure 5, we display the regions where $\psi_y^{(5)}$ is positive and negative for several choices of y. This confirms the "sinusoidal oscillation" of the sampling functions, in analogy with the sinc function.

The most striking feature of our data is the rapid decay of $\psi_y^{(m)}(x)$ as x moves away from y. Figure 6 shows the graph of the restriction of $\psi_y^{(5)}$ to a line segment in SG passing through y. To get a better understanding of what is going on, we have to examine the numerical data. We measure a crude distance $d_m(x, y)$ of x to y by the minimum number of cells of level m needed to connect x to y. In Table 1, we report the maximum (in absolute value) values of $\psi_y^{(m)}$ over all x of a given distance to y, for one choice of y for $m = 4$. We want to stress that the very small values that occur in Table 1 are the result of cancellation, as the individual summands in (2–4) are not themselves very small. The data, available in considerably finer detail on the web site, shows the same behavior for all y and $m \leq 5$.

Conjecture 3.1. *There exist constants c and $\alpha < 1$ (about 1/3) such that*

$$|\psi_y^{(m)}(x)| \leq c\alpha^{d_m(x,y)} \tag{3–1}$$

for all $y \in V_m \setminus V_0$, all $x \in SG$, and all m.

There is a natural metric $d_R(x, y)$, called the *resistance metric* (see [Kigami 01] for the precise definition) that is

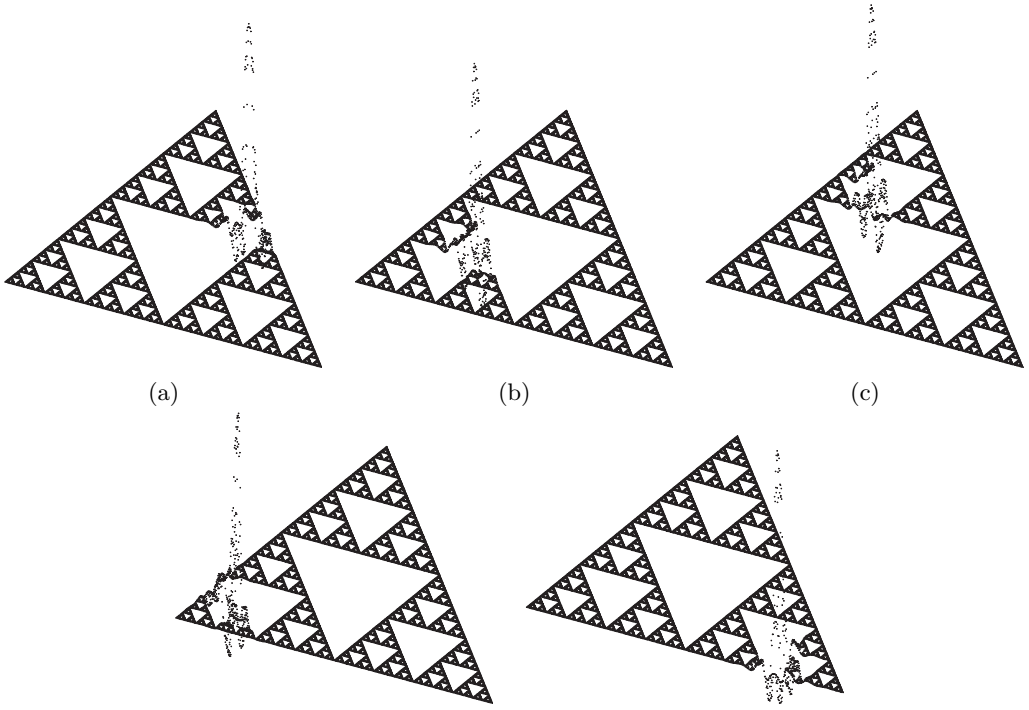

FIGURE 4. The graphs of $\psi_y^{(5)}$ for five choices of y in V_5.

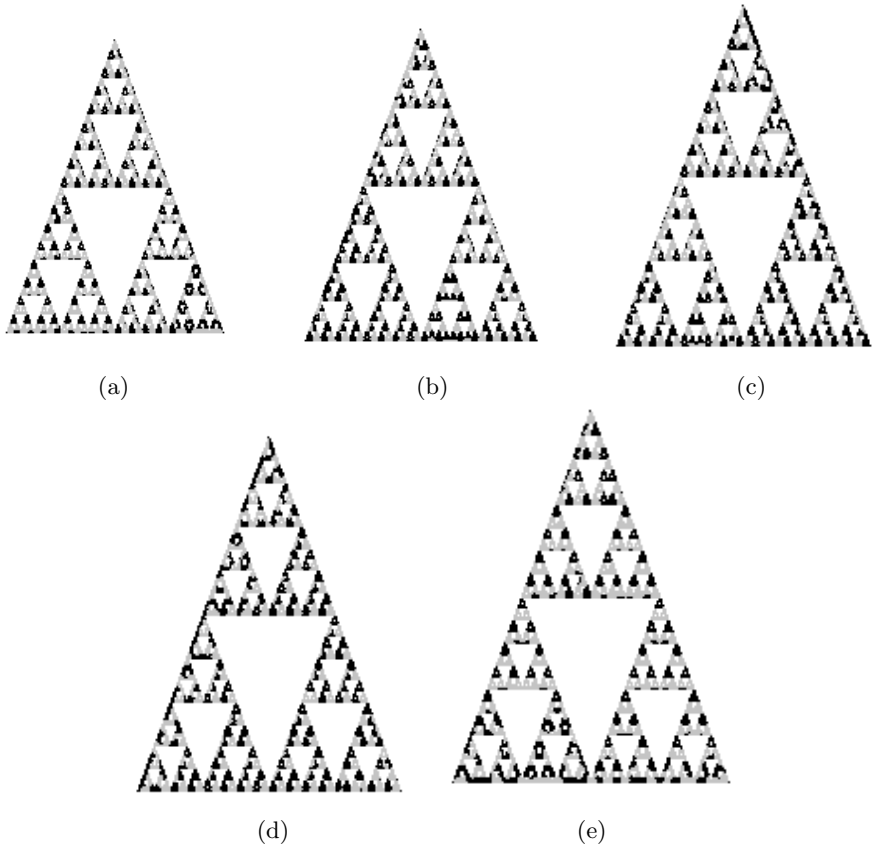

FIGURE 5. For each of the functions $\psi_y^{(5)}$ graphed in Figure 4, the regions where it is nonnegative (dark) and negative (light).

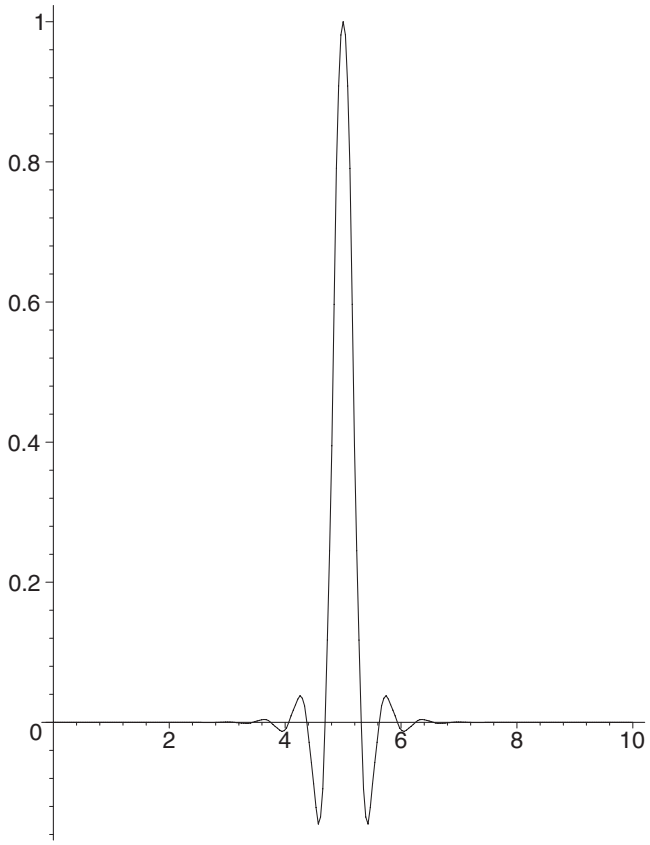

FIGURE 6. The graph of the restriction to a line segment of $\psi_y^{(5)}$ for y a point in $V_1 \setminus V_0$.

related to $d_m(x,y)$ by

$$d_m(x,y) \approx \left(\left(\frac{5}{3}\right)^m d_R(x,y)\right)^{\frac{\log 2}{\log(5/3)}}. \qquad (3\text{–}2)$$

In terms of this metric, (3–1) becomes

$$|\psi_y^{(m)}(x)| \le c_1 \exp\Big(- c_2\Big(\Big(\frac{5}{3}\Big)^m d_R(x,y)\Big)^{\frac{\log 2}{\log(5/3)}}\Big). \qquad (3\text{–}3)$$

Another way we can attempt to describe the sampling functions $\psi_y^{(m)}$ is as a sum of two terms, a main term that is independent of y, and a correction term that depends on y. Of course the different points $y \in V_m$ are not even locally isometric, so we can't exactly realize this goal. But it does appear that if we fix any y and then increase m, the behavior of $\psi_y^{(m)}$ in a neighborhood of y does approach, after appropriate rescaling, a function that might be called an *ideal spike*. In order to describe this function, we introduce the fractal blow-ups

$$\widetilde{SG}_i = \bigcup_{i=0}^{\infty} F_i^{-n}(SG)$$

distance to y	largest value (in absolute value)
1	1
2	-2.97983×10^{-1}
3	1.32806×10^{-1}
4	-4.38523×10^{-2}
5	1.36440×10^{-2}
6	-5.73710×10^{-3}
7	2.05985×10^{-3}
8	-2.69386×10^{-4}
9	9.43078×10^{-5}
10	-3.03346×10^{-5}
11	1.31507×10^{-5}
12	-3.78674×10^{-6}
13	1.34664×10^{-6}
14	-4.13866×10^{-7}
15	1.84896×10^{-7}

TABLE 1.

(increasing union). These are noncompact fractals with a single boundary point q_i (see [Strichartz 99]) and a reflection symmetry R_i that fixes q_i and interchanges q_{i-1} and q_{i+1}. Note that for $x \in (\widetilde{SG})_i$, $F_i^n x \in SG$ for all large enough n.

Conjecture 3.2. *Let $y \in F_w q_i \in V_m$, $|w| = m$. Then the following limit*

$$\lim_{n\to\infty} \psi_y^{(m+n)}(F_w F_i^n x) = \psi_i(x) \quad \textit{for} \quad x \in (\widetilde{SG})_i$$

exists and is independent of y. The ideal spikes ψ_i are R_i invariant and are equal under the obvious isomorphisms of $(\widetilde{SG})_i$.

We also computed the Dirichlet kernel $D_{d_m}(x,y)$ given by (1–12) for $1 \le m \le 5$. Note that these functions are defined on $SG \times SG$, so it is not sufficient to restrict y to V_m. It makes sense to fix one of the variables, say y, and study the behavior of D_{d_m} as a function of x. By abuse of notation, we will refer to $D_{d_m}(\cdot, y)$ as a Dirichlet kernel. We know that as $m \to \infty$, $D_{d_m}(\cdot, y)$ approaches the delta function at y in a weak sense. Our evidence indicates that $D_{d_m}(\cdot, y)$ resembles a delta function in a very strong sense, and that the choice $y \in V_m$ is very atypical (as explained below). In fact, we see the same sort of localization as for the sampling function. Figure 7 shows the graph of the Dirichlet kernel for $m = 5$ for two choices of y, one in V_5 and one not in V_5. Figure 8 shows the graph of the restriction of the first Dirichlet kernel from Figure 7 to a line passing through y. In Table 2, we report the same data as in Table 1 for a Dirichlet kernel with $m = 4$ for a particular choice of y. Note that the

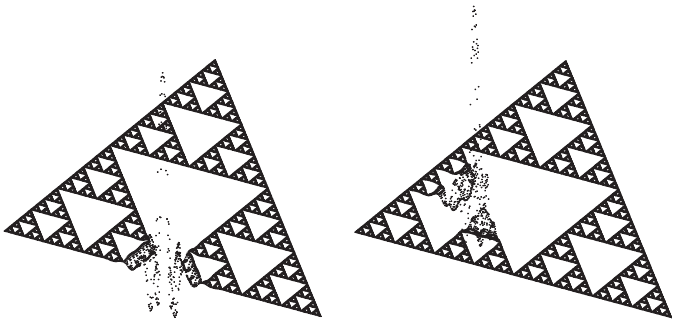

(a) (b)

FIGURE 7. The graph of two Dirichlet kernels for $m = 5$: (a) y in $V_1 \setminus V_0$, (b) y not in V_5.

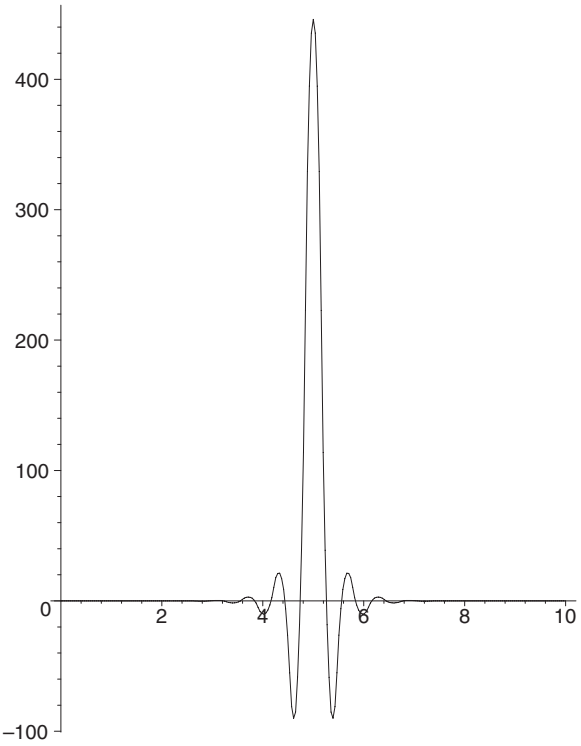

FIGURE 8. The graph of the restriction to a line segment of the Dirichlet kernel from Figure 7(a).

values at points near y are large, as we would expect for a delta function.

For each Dirichlet kernel, we computed three integrals:

$$\int |D_{d_m}(x,y)|^2 d\mu(x) \qquad (3\text{–}4)$$

$$\int |D_{d_m}(x,y)| d\mu(x) \qquad (3\text{–}5)$$

$$\int D_{d_m}(x,y) d\mu(x), \qquad (3\text{–}6)$$

which we refer to as the square of the L^2 norm, the L^1 norm, and the integral, respectively. We know from (1–12) that the average value of (3–4) as y varies is exactly d_m. We found that there is considerable variation in (3–4), and when $y \in V_m$ the values come out quite a bit higher than d_m (for example, when $m = 5$, the average value of (3–4) over all $y \in V_5$ was 405, compared with $d_m = 363$). This is the evidence that the Dirichlet kernels for $y \in V_m$ are atypical. To avoid this bias, we decided to look at Dirichlet kernels for y varying over 50 random points in V_8 (this was the limit of resolution for our computations). In Table 3, we give the average values over these 50 random points of the square of the L^2 norm, the L^1 norm, and the integral, for $m = 1, 2, 3, 4, 5$.

distance to y	largest value (in absolute value)
1	127.915
2	−35.0002
3	23.1213
4	−14.1982
5	1.85918
6	−1.38444
7	3.79040×10^{-1}
8	-1.47526×10^{-1}
9	3.15423×10^{-2}
10	-2.30019×10^{-2}
11	4.08147×10^{-3}
12	-2.42384×10^{-3}
13	4.77844×10^{-4}
14	-3.65649×10^{-4}
15	9.58635×10^{-5}
16	-4.19123×10^{-5}

TABLE 2.

m	d_m	square of L^2 norm	L^1 norm	integral
1	3	2.87645	1.26962	.90388
2	12	12.08358	1.98981	.97839
3	39	38.14721	2.18412	.98894
4	120	122.79748	2.31967	1.00513
5	363	355.08908	2.37096	1.00136

TABLE 3.

Comparing Tables 2 and 1, we see that the Dirichlet kernel exhibits a similar decay pattern as the sampling function, except that since the initial values near the diagonal are around d_m, we expect that the estimates (3–1) or (3–3) would be multiplied by d_m. This would yield an estimate for the Dirichlet kernel that is almost the same as for the heat kernel, with time $t \approx 5^{-m}$. Indeed, the heat kernel upper bound [Kigami 01] is a multiple of

$$t^{-\frac{\log 5}{\log 3}} \exp\Big(- c\Big(t^{-\frac{\log 5/3}{\log 5}} d_R(x,y)\Big)^{\frac{\log 5}{\log 3}}\Big), \qquad (3\text{–}7)$$

which for $t \approx 5^{-m}$ becomes

$$3^m \exp\Big(- c\Big(\Big(\frac{5}{3}\Big)^m d_R(x,y)\Big)^{\frac{\log 5}{\log 3}}\Big). \qquad (3\text{–}8)$$

Since $d_m \approx c3^m$, the difference between (3–8) and the right side of (3–3) multiplied by d_m is just in the power inside the exponential. In fact, such distinctions are too fine to be made on the basis of our data.

We are able to offer a heuristic argument why the Dirichlet kernel should resemble the heat kernel in this case. The heat kernel may be written, similarly to (1–12) as

$$\sum_{j=1}^{\infty} e^{-t\lambda_j} \widetilde{u}_j(x)\widetilde{u}_j(y), \qquad (3\text{–}9)$$

where λ_j denotes here the eigenvlaue of $\widetilde{u}_j$. Now it happens that the eigenvalues are changing dramatically around $j = d_m$. When $m = 2$ and $d_m = 12$, we have $\lambda_{12} = 677.859$, while the eigenvalue just below it is 279.429, and the eigenvalue just above it is 861.823 [Gibbons et al. 01], and these values are simply multiplied by 5^{m-2} when $m \geq 2$ (the case $m = 1$ is exceptional). Thus, by choosing $t = c5^{-m}$ for the appropriate choice of c, we can make the factors $e^{-t\lambda_j}$ close to zero for $j > d_m$ and close to one for $j \leq d_m$, so that (3–9) and (1–12) are not so different. This argument seems unconvincing when $j = d_m$, but here we observe that all the eigenfunctions associated with this eigenvalue are localized (supported in the union of two adjacent cells of order m), so they play no role in the off diagonal decay estimates we are considering. Of course, the argument we have presented is entirely heuristic, and there does not seem to be any hope that it can be transformed into a proof.

The data presented in Table 3 is also very interesting. The discrepancy between the values of d_m and the average square of the L^2 norm indicates that we would need to take considerably more than 50 random points to get more reliable results (the computations we did required several days of computer time, so it was not feasible to do much more). The expected value for the integral should approach one as $m \to \infty$, and the data is consistent with this. What is really startling is the small size of the average values of the L^1 norm. This is the analog of the Lebesgue constants in the theory of Fourier series. If we had analogous behavior, we would expect values on the order of $\log d_m = cm$, and clearly we are doing much better than that. The data is consistent with uniform boundedness for all the integrals (3–5) for all y and all m. (Additional evidence for this is the fact that the maximum value of the L^1 norm over all 50 random points is 2.70457 for $m = 4$ and 2.70901 for $m = 5$.) This would imply the uniform convergence of the partial sums, along the subsequence d_m, for the eigenfunction expansion of any continuous function vanishing on the boundary. On the basis of our data, we can only speculate on this possibility. Not only do we have the inaccuracy due to the small number of random points chosen, but it would be difficult to imagine an experiment that could distinguish between uniform boundedness and slow growth on the order of $\log\log d_m$.

It makes sense to consider also Dirichlet kernels $D_N(x,y)$ of orders N other than d_m, as long as we do not split multiple eigenvalues. In other words, we take the sum (1–12) up to $j = N$. It is easy to see that we could not possibly have the same sort of localization holding for all allowable choices of N, because as we change N at eigenvalues without multiplicity we add on nonlocalized terms. It remains poossible that some choices of N other than d_m might yield localization. Indeed, we argued above that the λ_{d_m} eigenfunctions are all localized, so if we chose the value of N just below d_m (this is not $d_m - 1$ because λ_{d_m} is an eigenvalue of high multiplicity), we would get the identical localization. We experimented by computing Dirichlet kernels D_N for all the allowable values $N = 45, 46, 48.50, 51, 54, 57, 60, 61, 63, 65, 66, 81$ between $d_3 = 39$ and $d_4 = 120$, and found that $N = 81$ just below d_4 was the only one to exhibit any localization.

(Note added March 2003: Further experimental work of Kealey Dias (http://www.mathlab.cornell.edu/∼dias) indicates the existence of a Gibbs' phenomenon for $N = d_m$. This is reported in [Coletta et al. 03].)

4. SAMPLING APPROXIMATION

The sampling formula (2–2) is exact for bandlimited functions, but it can also be used as an approximation formula for more general functions. In order to assert that this is a useful method of approximation, one would have to show that the error is small for reasonable classes

m	upper bound for $M_m(x)$
1	1.894427
2	2.469615
3	2.716993
4	2.749244

TABLE 4.

of functions, and that the sampling approximation is easier to manipulate than the original function in solving specific problems. In this section, we will present experimental evidence that the error is indeed small for a large class of functions. It seems plausible that the sampling approximation may form the basis of a new approach to numerical analysis on SG for solving various classes of fractal differential equations, but more work will be needed to carry this out. It is not clear whether or not sampling approximation can outperform the spline-based numerical methods of [Strichartz and Usher 00] and [Gibbons et al. 01].

The key to understanding the approximation error is to estimate the functions

$$\sum_{y\in V_m\setminus V_0} |\psi_y^{(m)}(x)| = M_m(x). \tag{4–1}$$

In Table 4, we display the upper bounds we have found experimentally.

Conjecture 4.1. *The functions $M_m(x)$ are uniformly bounded by 2.8 for all m.*

In Figure 9, we display the graph of the function $M_4(x)$. Note that $M_m(x) = 1$ for $x \in V_m \setminus V_0$.

If f is any continuous function vanishing on V_0, write

$$S_m f(x) = \sum_{y\in V_m\setminus V_0} f(y)\psi_y^{(m)}(x) \tag{4–2}$$

for its sampling approximation of level m. If

$$f(x) = \sum_{j=1}^{\infty} c_j \widetilde{u}_j \tag{4–3}$$

is its expansion in terms of an orthonormal basis $\{\widetilde{u}_j\}$ of Dirichlet eigenfunctions, write

$$f = f_m + f^m \tag{4–4}$$

for

$$f_m(x) = \sum_{j=1}^{d_m} c_j \widetilde{u}_j(x). \tag{4–5}$$

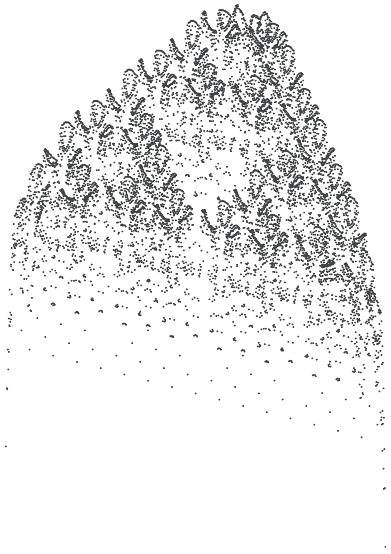

FIGURE 9. The graph of $M_4(x)$.

Then $S_m f_m = f_m$ so

$$S_m f - f = S_m f^m - f^m. \tag{4–6}$$

Under various hypotheses on f, we can conclude that f^m is small. For example, if we just assume that f has finite energy, this means

$$\mathcal{E}(f,f) = \sum_{j=1}^{\infty} |c_j|^2 \lambda_j < \infty, \tag{4–7}$$

hence $\mathcal{E}(f^m, f^m) \to 0$ as $m \to \infty$. Since

$$\|f\|_\infty \le c\mathcal{E}(f,f)^{1/2} \tag{4–8}$$

for any f vanishing on V_0, we have $f^m \to 0$ uniformly as $m \to \infty$. But

$$|S_m f^m(x)| \le M_m(x)\|f^m\|_\infty \tag{4–9}$$

hence, $S_m f \to f$ uniformly under Conjecture 4.1.

We can obtain a rate of convergence if we assume f belongs to the domain of Δ (or $\mathrm{dom}_{L^2}\Delta$). For then

$$\begin{aligned}\mathcal{E}(f^m, f^m) &= \sum_{j=d_m+1}^{\infty} |c_j|^2\lambda_j \le (\lambda_{d_m+1})^{-1} \\ &\quad \times \sum_{j=1}^{\infty} |\lambda_j c_j|^2 \\ &= (\lambda_{d_m+1})^{-1}\|\Delta f\|_2^2 \end{aligned} \tag{4–10}$$

and $\lambda_{d_m} = c5^m$. Thus,

$$\|f^m\|_\infty \le c5^{-m/2} \tag{4–11}$$

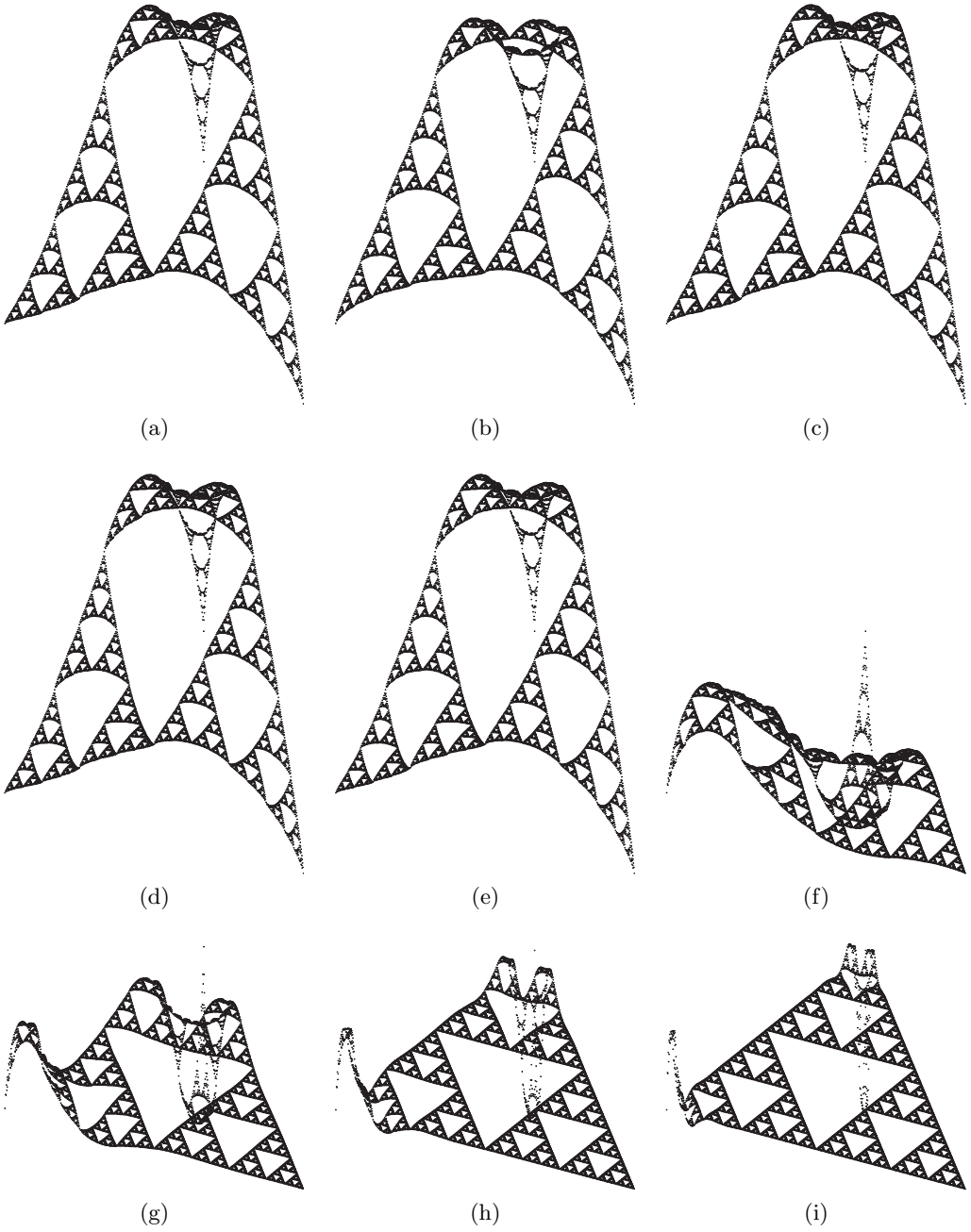

FIGURE 10. Graphs of (a) the function f_1, (b)–(e) the approximations of orders $m = 1, 2, 3, 4$, and (f)–(i) the differences (the vertical axis scale is not the same for all m).

by (4–8) and (4–10), which implies

$$\|S_m f - f\|_\infty \le c M_m 5^{-m/2}, \tag{4–12}$$

where $M_m = \|M_m(x)\|_\infty$. (Incidentally, we cannot improve the estimated rate of convergence by assuming more "smoothness" for f in the form of f belonging to the domain of higher powers of the Laplacian, because we do not have

$$(-\Delta)^k f = \sum_{j=1}^{\infty} \lambda_j^k c_j \widetilde{u}_j$$

for $k > 1$ without imposing rather artificial boundary conditions.)

In typical applications of sampling approximation, one would not be dealing with large values of m, so these

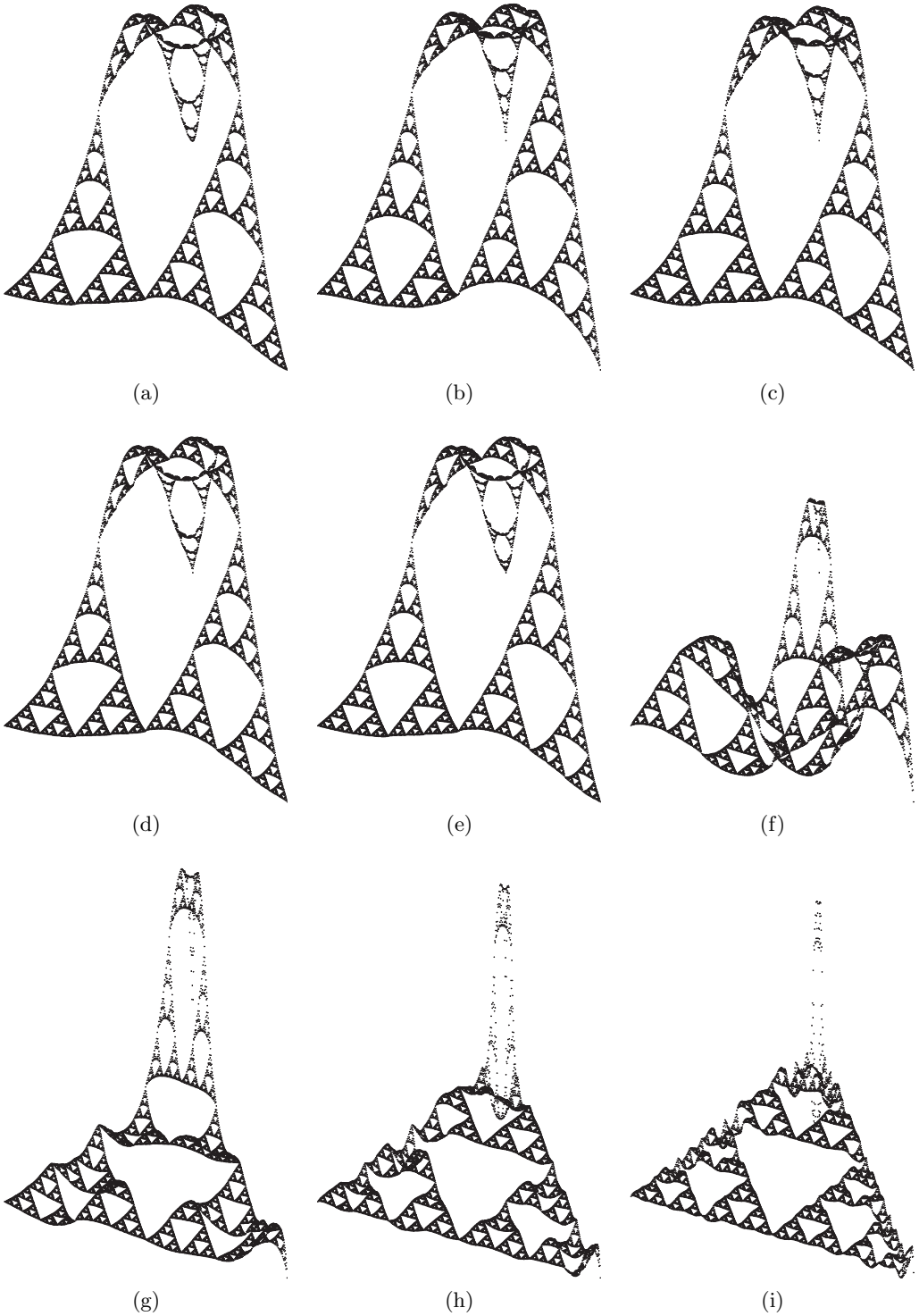

FIGURE 11. The graphs of (a) the function f_2, (b)–(e) the approximations of orders $m = 1, 2, 3, 4$, and (f)–(i) the differences (the vertical axis scale is not the same for all m).

m	Max error f_1	Max error f_2
1	.228945	.448683
2	.044125	.405737
3	.008813	.136708
4	.001763	.045786

TABLE 5.

estimates may be beside the point. We did some tests of the method that suggest that it is very effective, not only in the size of the maximum error, but also in the ability of the approximation to capture the qualitative features of the function. Generally speaking, the more rapidly the function oscillates, the larger one would have to take m in order to have a reasonable approximation. Since we are not equipped to handle large values of m, we restricted our test to functions with slow oscillation. The first function we chose, f_1, is a biharmonic function ($\Delta^2 f_1 = 0$) vanishing on V_0, an example of an infinitely smooth function. The second function, f_2, is the square of f_1, which means that it has finite energy, but does not belong to $\mathrm{dom}_{L^2}\Delta$ [Ben Bassat et al. 99]. We have $\|f_1\|_\infty \approx 1.7$ and $\|f_2\|_\infty \approx 3$.

In Table 5, we report the maximum error of approximation.

In Figure 10, we display the graphs of f_1 and its approximations, as well as the errors. Figure 11 does the same for f_2. It is striking that the largest errors occur near the boundary, and away from a small neighborhood of the boundary the error is substantially smaller than the maximum error. In particular, the average error should be an order of magnitude better than the maximum error. Also note that already by $m = 2$, even though the numerical error is significant, the graph of the approximation appears to be almost identical to the graph of the function, except for the behavior near to boundary points. (The fact that one boundary point is much better than the other two has to do with the specific choice of function, namely its normal derivative vanishes at that point.)

5. IRREGULAR SAMPLING

In this section, we consider the question of changing the sampling set V_m while keeping the bandlimited space B_m. Specifically, we ask which sets S of cardinality d_m have the property that the restriction of functions in B_m to S remains a space of dimension d_m. This is equivalent to the nonvanishing of

$$\det\{\psi_y^{(m)}(x)\}_{x\in S, y\in V_m\setminus V_0}, \qquad (5\text{–}1)$$

which implies the existence of sampling functions $\psi_y^{(S)}(x)$ for each $y \in S$ such that the sampling formula (2–2) holds for B_m. In the case of regular sampling, $S = V_m \setminus V_0$, the determinant (5–1) is one. Although any nonzero value for (5–1) allows sampling, we want to avoid very small values as this may lead to "unstable" sampling formulas with very large functions $\psi_y^{(S)}$ that may unduly amplify sampling errors.

Unlike the case of the unit interval, not every set S of d_m distinct points will do. The space B_m contains localized eigenfunctions supported on any pair of adjacent $m-1$ cells, so every sampling set S must contain at least one point in the interior of every pair of adjacent $m-1$ cells (the interior contains the intersection point of the cells, but not the other boundary points of the cells). It is conceivable that the converse is true, but we have not tested it directly.

We have looked at the idea that a reasonable perturbation of $V_m \setminus V_0$ is always a sampling set, with a specific lower bound on (5–1). Points $y \in V_m \setminus V_0$ have a natural system of neighborhoods $U_n(y)$, for $n \geq m$, consisting of the union of the two n cells containing y as a boundary point. A set S is called an (m, n) *perturbation* of $V_m \setminus V_0$ if S consists of one point $\widetilde{y}$ from $U_n(y)$ for each $y \in V_m \setminus V_0$. Let $\delta(m, n)$ denote the minimum value of (5–1) as S varies over all (m, n) perturbations of $V_m \setminus V_0$. It appears that we can compute $\delta(m, n)$ for moderate values of m and n. We can easily compute the determinant (5–1) for any choice of S, but there are infinitely many perturbations, so we can't search all possibilities. A reasonable compromise is to search all possibilities where $\widetilde{y}$ is restricted to V_k points in $U_n(y)$ for k moderately larger than n. Rather serendipitously, we found that it suffices to take $k = n$, since the minimum value never changed when we increased k above n. In other words, an extremal perturbation apparently always exists with each $\widetilde{y}$ equal to one of the five V_n points in $U_n(y)$ (the boundary points of the two n cells). If this observation is indeed always true, then the computation of $\delta(n, m)$ only requires a search of 5^{d_m} possible perturbations.

	$m=1$	$m=2$	$m=3$
$n=2$	0		
$n=3$	.681045	0	
$n=4$	.910845	.134638	0
$n=5$	.973817	.550821	.003733
$n=6$	.991750	.791145	.248726
$n=7$	.997262	.895151	.619498
$n=8$	.999061	.943220	.824522

TABLE 6.

In Table 6, we report the values of $\delta(m,n)$ for $m = 1,2,3$ and $m+1 \le n \le 8$.Note that $\delta(m,m+1) = 0$ because the neighborhoods $U_{m+1}(y)$ overlap at points.

Conjecture 5.1.

(a) $\delta(m,n) > 0$ for $n \ge m+2$, so in particular every $(m,m+2)$ perturbation of V_m is a sampling set for B_m.

(b) There is a uniform lower bound (about .134638) for $\delta(m,2m)$ for $m \ge 2$.

It seems clear that we will not get a uniform lower bound for $\delta(m,m+k)$ for all m for any fixed k. On the other hand, one might be able to improve (b) by taking $\delta(m,[\lambda m])$ for a fixed constant $\lambda > 1$ (changing the lower bound, of course). Perhaps any $\lambda > 1$ would suffice.

ACKNOWLEDGMENTS

Research of Richard Oberlin and Brian Street was supported by the National Science Foundation through the Research Experiences for Undergraduates Program at Cornell. Research of Robert S. Strichartz was supproted in part by the National Science Foundation Grant DMS 9970337.

REFERENCES

[Barlow 98] M. Barlow. "Diffusion on fractals." In *Lectures on Probability and Statistics*, Lecture Notes Math., 1690, pp. 1–121. Berlin: Springer-Verlag, 1998.

[Barlow and Kigami 97] M. Barlow and J. Kigami. "Localized Eigenfunctions of the Laplacian on p.c.f. Self-Similar Sets." *J. London Math. Soc.* 56 (1997), 320–332.

[Ben Bassat et al. 99] O. Ben-Bassat, R. Strichartz, and A. Teplyaev. "What Is Not in the Domain of the Laplacian on Sierpinski Gasket Type Fractals." *Journal of Functional Analysis* 166 (1999), 197–217.

[Benedetto and Ferreira 01] J. J. Benedetto and P. J. S. G. Ferreira, editors. *Modern Sampling Theory.* Boston, MA: Birkhauser, 2001.

[Cauchy 41] A. Cauchy. "Mémoire sur diverses formules d'analyse." *Comptes Rendue Acad. Sci. Paris* (12) (1841), 283–298; (reprinted in *Oeuvres Complète d'Augustin Cauchy*, Series 1, Vol. 6, Extract Number 118, 63–78, Paris: Gauthier-Villars, 1888)

[Coletta et al. 03] K. Coletta, K. Dias, and R. Strichartz. "Numerical Analysis on the Sierpinski Gasket, with Applications to Schrödinger Equations, Wave Equation, and Gibbs' Phenomenon." Preprint, 2003.

[Dalrymple et al. 99] K. Dalrymple, R. Strichartz, and J. Vinson. "Fractal Differential Equations on the Sierpinski Gasket." *J. Fourier Anal. Appl.* 5 (1999), 203–284.

[Fukushima and Shima 92] M. Fukushima and T. Shima. "On a Spectral Analysis for the Sierpinski Gasket." *Potential Anal.* 1 (1992), 1–35.

[Gibbons et al. 01] M. Gibbons, A. Raj, and R. Strichartz. "The Finite Element Method on the Sierpinski Gasket." *Constructive Approx.* 17 (2001), 561–588.

[Kigami 89] J. Kigami. "A Harmonic Calculus on the Sierpinski Gasket." *Japan J. Appl. Math.* 6 (1989), 259–290

[Kigami 01] J. Kigami. *Analysis on Fractals.* Cambridge, UK: Cambridge University Press, 2001.

[Shima 96] T. Shima. "On Eigenvalue Problems for Laplacians on p.c.f Self-Similar Sets." *Japan J. Indust. Appl. Math.* 13 (1996), 1–23.

[Strichartz 96] R. Strichartz. "Fractals in the Large." *Can. Math. J.* 50 (1996), 638–657.

[Strichartz 99] R. Strichartz. "Analysis on Fractals." *Notices American Mathematical Society* 46 (1999), 1199–1208.

[Strichartz and Usher 00] R. Strichartz and M. Usher. "Splines on Fractals." *Math. Proc. Cambridge Phil. Soc.* 129 (2000), 331.

Richard Oberlin, Math Dept., Florida State University, Tallahassee, FL 32306
(Current address: Mathematics Department, University of Wisconsin, Madison, WI 53706) (oberlin@math.wisc.edu)

Brian Street, Math Department, Fine Hall, Princeton University, Princeton, NJ 08544 (bstreet@math.princeton.edu)

Robert S. Strichartz, Mathematics Department, Malott Hall, Cornell University, Ithaca, NY 14853 (str@math.cornell.edu)

Received April 30, 2002; accepted March 20, 2003.